Original Article

The SUMO Conjugating Enzyme Ubc9 is a Regulator of GLUT4 Turnover and Targeting to the Insulin-Responsive Storage Compartment in 3T3-L1 Adipocytes

Li-Bin Liu, Waka Omata, Itaru Kojima, and Hiroshi Shibata

The small ubiquitin-related modifier (SUMO) conjugating enzyme Ubc9 has been shown to upregulate GLUT4 in L6 myoblast cells, although the mechanism of action has remained undefined. Here we investigated the physiological significance of Ubc9 in GLUT4 turnover and subcellular targeting by adenovirus vector–mediated overexpression and by small interfering RNA (siRNA)-mediated gene silencing of Ubc9 in 3T3-L1 adipocytes. Overexpression of Ubc9 resulted in an inhibition of GLUT4 degradation and promoted its targeting to the unique insulin-responsive GLUT4 storage compartment (GSC), leading to an increase in GLUT4 amount and insulin-responsive glucose transport in 3T3-L1 adipocytes. Overexpression of Ubc9 also antagonized GLUT4 downregulation and its selective loss in GSC induced by long-term insulin stimulation. By contrast, siRNA-mediated depletion of Ubc9 accelerated GLUT4 degradation and decreased the amount of the transporter, concurrent with its selective loss in GSC, which resulted in attenuated insulin-responsive glucose transport. Intriguingly, overexpression of the catalytically inactive mutant Ubc9-C93A produced effects indistinguishable from those with wild-type Ubc9, suggesting that Ubc9 regulates GLUT4 turnover and targeting to GSC by a mechanism independent of its catalytic activity. Thus, Ubc9 is a pivotal regulator of the insulin sensitivity of glucose transport in adipocytes. *Diabetes* 56:1977–1985, 2007

From the Department of Cell Biology, Institute for Molecular and Cellular Regulation, Gunma University, Maebashi, Japan.

Address correspondence and reprint requests to Hiroshi Shibata, MD, PhD, Department of Cell Biology, Institute for Molecular and Cellular Regulation, Gunma University, 3-39-15 Showa-machi, Maebashi 371-8512, Japan. E-mail: hshibata@showa.gunma-u.ac.jp.

Received for publication 8 August 2006 and accepted in revised form 19 May 2007.

Published ahead of print at http://diabetes.diabetesjournals.org on 29 May 2007. DOI: 10.2337/db06-1100.

L.-B.L. and W.O. contributed equally to this work.

ALLM, *N*-acetyl-Leu-Leu-Met-CHO; C/EBP, CCAAT/enhancer-binding protein; CHO, Chinese hamster ovary; CHO-IR, CHO cells expressing the insulin receptor; CHO-IR-GLUT4, CHO cells expressing the insulin receptor and GLUT4; DMEM, Dulbecco's modified Eagle's medium; FBS, fetal bovine serum; GFP, green florescent protein; GSC, GLUT4 storage compartment; IRAP, insulin-regulated aminopeptidase; LDM, low density membrane; M6PR, mannose-6-phosphate receptor; PPAR, peroxisome proliferator–activated receptor; siRNA, small interfering RNA; SNARE, soluble *N*-ethylmaleimide-sensitive factor attachment protein receptor; SUMO, small ubiquitin-related modifier; TGN, trans-Golgi network.

The glucose transport system of muscle and adipose cells is unique in that its activity is rapidly upregulated by 10- to 40-fold upon insulin stimulation, mainly by recruiting the insulin-regulated glucose transporter GLUT4 from intracellular compartments to the plasma membrane (1–4). While such a robust response to insulin of glucose transport coincides with the expression of GLUT4 during differentiation of muscle and adipose cells (5,6), GLUT4 expression is not sufficient to confer insulin sensitivity to glucose transport system in other cell types such as fibroblasts or Chinese hamster ovary (CHO) cells (7–9). Thus, in addition to GLUT4 expression, another factor(s) may be required for acquisition of the insulin sensitivity of glucose transport. In this regard, GLUT4 is localized mainly to the recycling compartments when ectopically expressed in those insulin-insensitive cells (10), whereas a significant portion of GLUT4 resides in a specialized storage compartment sequestered from the recycling pathways in muscles and adipocytes (rev. in 3,4). Thus, immuno-electron microscopic studies have demonstrated that insulin recruits GLUT4 to the plasma membrane from the tubulovesicular elements near the endosomes and trans-Golgi network (TGN) and scattered throughout the cytoplasm in adipocytes (11,12). In addition, biochemical ablation of endosomes is unable to deplete a significant portion (~60%) of GLUT4 in 3T3-L1 adipocytes (13,14). While insulin also elicits translocation of other recycling proteins such as GLUT1, the transferrin receptor, and the IGF-II/mannose 6-phosphate receptor (M6PR), the fold-stimulation of insulin is far less than that of GLUT4 (15–17). These observations suggest that GLUT4 targeting to the unique insulin-responsive storage compartments (referred to here as GSC) may be crucial for acquisition of the insulin-responsiveness of glucose transport. This was further supported by the recent study that GLUT4 targeting to GSC coincides with a dramatic increase in the responsiveness of glucose transport during differentiation of adipocytes (18).

On the other hand, Giorgino et al. (19) have identified Ubc9, the small ubiquitin-related modifier (SUMO) conjugating enzyme, as a GLUT4 and GLUT1 interactive protein. Overexpression of Ubc9 in L6 myoblasts upregulated ectopically expressed GLUT4 with a concurrent decrease in GLUT1 and potentiated the insulin-responsive glucose transport. While they argued that these effects of Ubc9 are brought about by SUMOylation of the glucose transporters, the precise mechanism of Ubc9 action has remained unclear. In addition, it has yet to be investigated whether

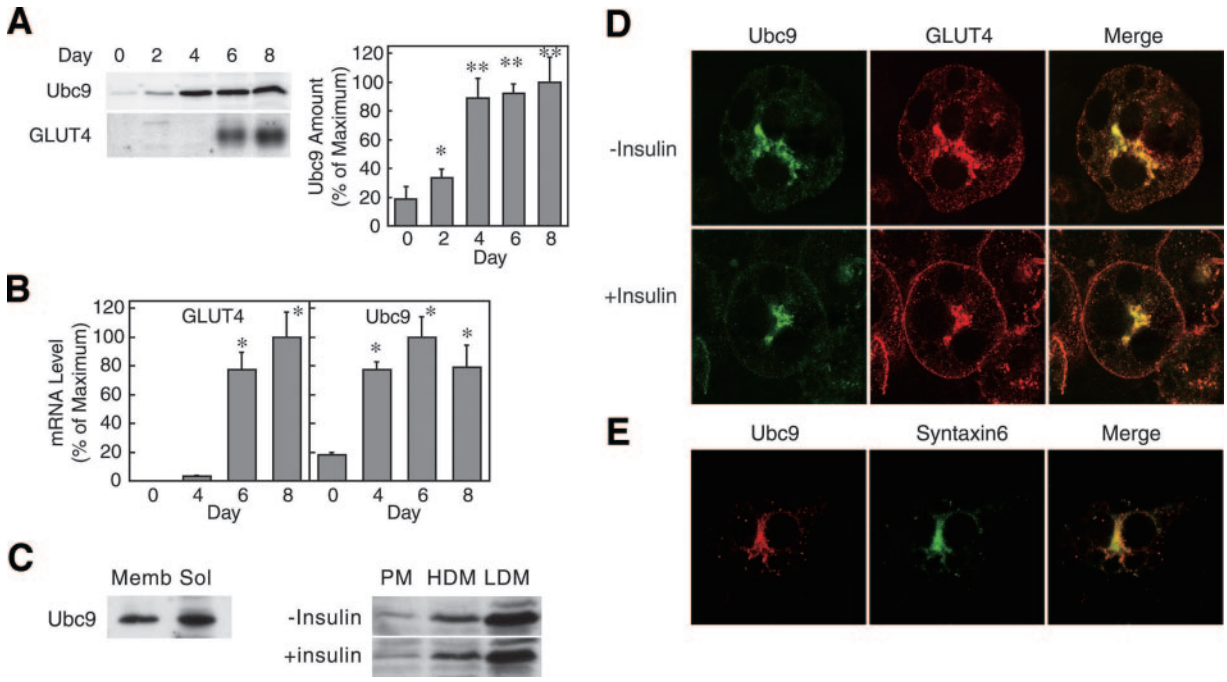

FIG. 1. Expression and localization of Ubc9 in 3T3-L1 adipocytes. *A*: 3T3-L1 preadipocytes were differentiated as described in RESEARCH DESIGN AND METHODS. At the indicated time points, cells were lysed and subjected to immunoblotting with anti-Ubc9 or anti-GLUT4 antibodies. The representative immunoblot data for Ubc9 and GLUT4 were shown (*left panel*). The relative amounts of Ubc9 were quantified and are shown as the mean ± SE (n = 3) (*right panel*). *P < 0.05; **P < 0.01 (vs. day 0). *B*: 3T3-L1 cells were differentiated and the mRNA levels of GLUT4 and Ubc9 were measured by quantitative real-time RT-PCR. Results are shown as the mean ± SE (n = 4). *P < 0.01 (vs. day 0). *C*: The plasma membrane, high-density microsome fraction and LDM fractions were prepared from differentiated 3T3-L1 adipocytes treated without or with insulin (100 nmol/l) for 30 min and subjected to immunoblotting with anti-Ubc9 antibody. HDM, high-density microsome fraction; LDM, low density microsome fraction; Memb, membrane fraction; PM, plasma membrane fraction; Sol, soluble fraction. *D*: The subcellular localization of Ubc9 and GLUT4 in 3T3-L1 adipocytes. Differentiated 3T3-L1 adipocytes stimulated without or with insulin (100 nmol/l) for 30 min were immunostained for GLUT4 (red) and Ubc9 (green) and the images obtained by confocal microscopy as described under RESEARCH DESIGN AND METHODS. *E*: The subcellular localization of Ubc9 (red) and Syntaxin6 (green) in 3T3-L1 adipocytes.

the observations in L6 myoblasts would be applicable to the physiological insulin-sensitive cells. Nevertheless, their study raised the possibilities that GLUT4 expression level may be regulated by posttranscriptional or posttranslational mechanisms and that Ubc9 may be a regulator of insulin sensitivity of glucose transport.

In the present study, by adenovirus-mediated overexpression and small interfering RNA (siRNA)-mediated knockdown of Ubc9, we investigated the physiological role of Ubc9 in 3T3-L1 adipocytes. We demonstrate here that Ubc9 is a crucial regulator of GLUT4 targeting and turnover in 3T3-L1 adipocytes and plays an indispensable role in the acquisition of insulin sensitivity of glucose transport.

RESEARCH DESIGN AND METHODS

Antibodies. Antibodies for GLUT4, GLUT1, insulin-regulated aminopeptidase (IRAP), vesicle-associated membrane protein-2 (VAMP-2), and syntaxin 4 were described previously (20,21). Anti–syntaxin 6 and anti-sortilin antibodies were obtained from Transduction Laboratories. Anti-Ubc9 antibody was from Oncogene Research Products. Anti-transferrin receptor and anti–SUMO-1 antibodies were from Zymed Laboratories. Anti-Akt and anti–phospho-Akt (Ser473) antibodies were from Cell Signaling Technology. Anti–peroxisome proliferator–activated receptor (PPAR)-γ, anti–CCAAT/enhancer-binding protein (C/EBP)-α, and anti-C/EBPβ antibodies were from Santa Cruz.

Cell culture. 3T3-L1 cells maintained in Dulbecco's modified Eagle's medium (DMEM) supplemented with 75 μg/ml penicillin, 100 μg/ml streptomycin, and 10% calf serum at 37°C in a humidified atmosphere of 5% CO_2 were differentiated into adipocytes as described by Student et al. (22). Briefly, 2 days after confluence, the medium was replaced with fresh medium containing 10% fetal bovine serum (FBS), 0.5 mmol/l 3-isobutyl-1-methylxanthine, 1 μmol/l dexamethasone, and 1.7 μmol/l insulin. Forty-eight hours later, the medium was replaced with fresh medium containing 10% FBS and 1.7 μmol/l insulin. After 48 h, cells were maintained in DMEM containing 10% FBS.

CHO cells expressing the insulin receptor and GLUT4 (CHO-IR-GLUT4) were maintained as described previously (23).

Retrovirus production and infection. Platinum-E ecotropic retrovirus packaging cells provided by Toshio Kitamura (University of Tokyo) were maintained in DMEM supplemented with 10% FBS, 1 μg/ml puromycin, 10 μg/ml blasticidine, 75 μg/ml penicillin, and 50 μg/ml streptomycin and transfected with the retrovirus vector pB–GLUT4–myc7–green florescent protein (GFP) provided by H.F. Lodish (Massachusetts Institute of Technology), using FuGene 6 transfection reagent (Roche Applied Science). Media containing recombinant retroviruses were harvested 24 h after transfection and used to infect 3T3-L1 preadipocytes. The recombinant retrovirus was expressed with an efficiency of >80% as assessed by GFP fluorescence.

Adenovirus vectors. The cDNA for mouse Ubc9 was provided by René Bernards (the Netherlands Cancer Institute). The C93A mutation was introduced by using the QuickChange II Site-Directed Mutagenesis Kit (Stratagene). The recombinant adenoviruses encoding either wild-type or C93A mutant Ubc9 were generated using the ViraPower Adenoviral Expression System (Invitrogen) according to the manufacturer's instructions. The recombinant adenoviruses were amplified in 293 cells and purified by CsCl gradient centrifugation. Either 3T3-L1 adipocytes or CHO-IR-GLUT4 cells were infected with the virus at the MOI (multiplicities of infection) as indicated. The efficiency of adenovirus-mediated gene transfer was >90% at an MOI of 50 pfu/cell as measured by histocytochemical staining for β-galactosidase in LacZ-infected cells.

Quantitative RT-PCR. Total RNA was extracted from 3T3-L1 cells using the TRIzol reagent (Life Technologies) and transcribed into cDNA. Quantitative PCR was conducted in 20-μl reactions containing SYBR Premix Ex Taq (Takara Bio) using the ABI PRISM 7700 sequence detection system (Applied Biosystems). The oligonucleotide primers for mouse GLUT4, GLUT1, Ubc9, and β-actin were purchased from Takara Bio. Reaction mixtures were incubated for an initial denaturation at 95°C for 10 s, followed by 40 PCR cycles. Each cycle consisted of 95°C for 5 s and 60°C for 30 s. The mRNA levels of all genes were normalized using β-actin as internal control.

RNA interferance. Ubc9 siRNA and control (nonsilencing) siRNA were purchased from Qiagen. The sequence of the Ubc9 siRNA was targeted to base pairs 389–409 of the mouse Ubc9 cDNA. The dsRNA oligonucleotides used were 5′-AAGCAGAGGCCTACACAATdTdT-3′ (sense) and 5′-AAATTGTGTAG

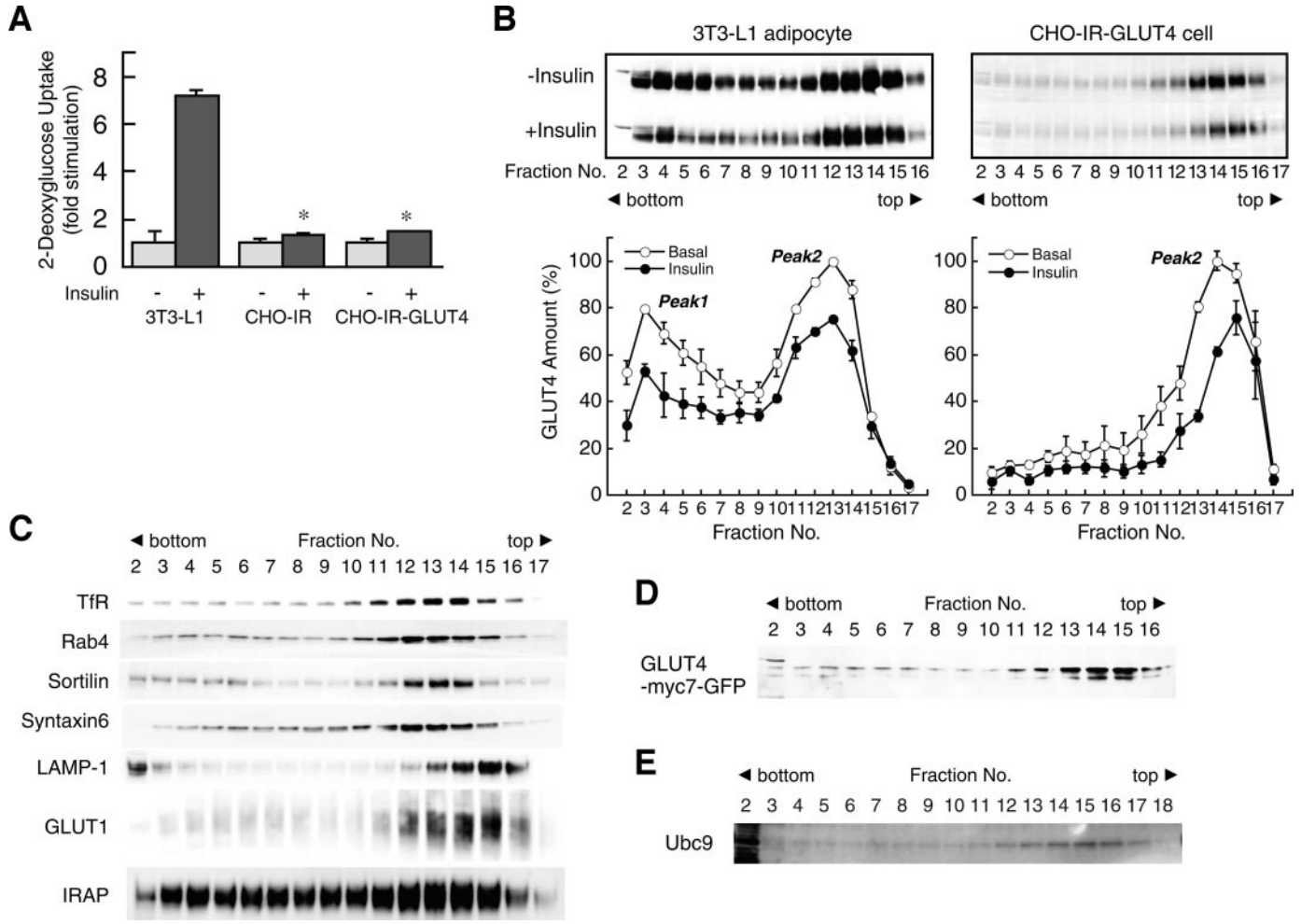

FIG. 2. Insulin-responsive glucose transport and subcellular distribution of GLUT4. *A*: Effects of insulin on glucose transport activity. Differentiated 3T3-L1 adipocytes, CHO-IR cells, or CHO-IR-GLUT4 cells in 12-well plates were stimulated without or with 100 nmol/l insulin for 30 min. Then the glucose transport activity was measured as described under RESEARCH DESIGN AND METHODS. Results are shown as the mean ± SE (n = 3–6) of the fold-stimulation over the basal transport activity. *P < 0.01 (vs. plus insulin value in 3T3-L1 adipocytes). *B*: Iodixanol gradient analysis of the subcellular distribution of GLUT4. 3T3-L1 adipocytes or CHO-IR-GLUT4 cells were stimulated with or without 100 nmol/l insulin for 30 min at 37°C. The LDM fractions were prepared and subjected to iodixanol gradient centrifugation as described in RESEARCH DESIGN AND METHODS. Fractions were collected and immunoblotted with an anti-GLUT4 antibody. The representative immunoblot data (*upper panels*) and the relative amounts of GLUT4 are shown as the percentage of the peak value of peak 2 in the basal cells (*lower panels*). Results are shown as the mean ± SE (n = 3). *C*: Distribution of various proteins in 3T3-L1 adipocytes. The LDM fraction from 3T3-L1 adipocytes was separated by iodixanol gradient centrifugation, and the fractions were subjected to immunoblotting with the indicated antibodies. TfR, transferrin receptor. *D*: Distribution of GLUT4-myc7-GFP in 3T3-L1 preadipocytes. The LDM fraction was obtained from 3T3-L1 preadipocytes expressing GLUT4-myc7-GFP and subjected to iodixanol gradient analysis. The fractions were immunoblotted for GLUT4. *E*: The iodixanol gradient fractions obtained from 3T3-L1 adipocytes were immunoblotted with anti-Ubc9 antibody.

GCCTCTGCdTdT-3′ (antisense). 3T3-L1 adipocytes were transfected with either control or Ubc9 siRNA by using RNAiFect reagent (Qiagen).

Measurement of GLUT4 turnover. Cells in a 60-mm dish were washed and incubated in methionine-free DMEM for 30 min at 37°C, followed by pulse-labeling in methionine-free DMEM containing 5% dialysed FBS and 110 μCi/dish of [^{35}S]methionine (PerkinElmer Life Sciences) for 12 h. The cells were washed with PBS and incubated in complete DMEM supplemented with 10% FBS and 100 μg/ml of L-methionine.

The labeled cells were washed with ice-cold PBS and homogenized in 1 ml lysis buffer (150 mmol/l NaCl, 1.0% NP-40, 0.1% SDS, 1 mmol/l EDTA/Na, and 50 mmol/l Tris/Cl, pH 8.0), followed by centrifugation at 12,000*g* for 10 min at 4°C. The supernatant was precleared by incubation for 2 h at 4°C with 40 μl protein A-Sepharose beads (50% vol/vol) loaded with rabbit nonimmune serum. The beads were sedimented by centrifugation and the supernatant incubated with 10 μl rabbit anti-GLUT4 or nonimmune serum for 1 h at 4°C. Then 40 μl protein A-Sepharose beads were added and the incubation continued overnight. The beads were washed once with lysis buffer containing 0.5% NP-40, once with lysis buffer containing 1 mol/l NaCl, twice with lysis buffer containing 0.5% NP-40, and once with PBS. The proteins were eluted from the beads by incubation in SDS sample buffer for 1 h at 37°C and subjected to SDS-PAGE and autoradiography using the BAS-1800 II bioimaging analyzer (Fuji Photo Film). The GLUT4 bands were identified by immunoblotting the lysate of unlabeled cells. The radioactivities of the GLUT4 bands were quantified with Image Gauge software (Fuji Photo Film). The radioactivity of immunoprecipitated GLUT4 was calculated by subtracting the radioactivity obtained with nonimmune serum.

Subcellular membrane fractionation. Cells were homogenized in ice-cold STE buffer (250 mmol/l sucrose, 10 mmol/l Tris/Cl, pH 7.4, and 1 mmol/l EDTA) and subjected to subcellular fractionation as described previously (20).

Iodixanol gradient analysis. Cells were washed and homogenized in ice-cold HES buffer (20 mmol/l HEPES/Na, pH 7.4, 1 mmol/l EDTA, and 250 mmol/l sucrose) containing complete protease inhibitor cocktail (Roche Diagnostics). The low density membrane (LDM) fraction prepared as described above was resuspended in HES buffer containing 14.0% (vol/vol) iodixanol solution. After centrifugation in a 5-ml sealed tube at 4°C with P100-VT vertical rotor (Hitachi) at 265,000*g* for 2.5 h with brake free, fractions (0.3 ml) were collected starting from the bottom of the tube.

Immunoblotting. Cells were homogenized in PBS containing complete protease inhibitor cocktail, followed by centrifugation for 5 min at 5,000 rpm at 4°C. The supernatant was subjected to immunoblotting as described previously (21). The blots were visualized by using enhanced chemiluminescence or the ECL plus system (Amersham Biosciences) and LAS-3000 lumi-

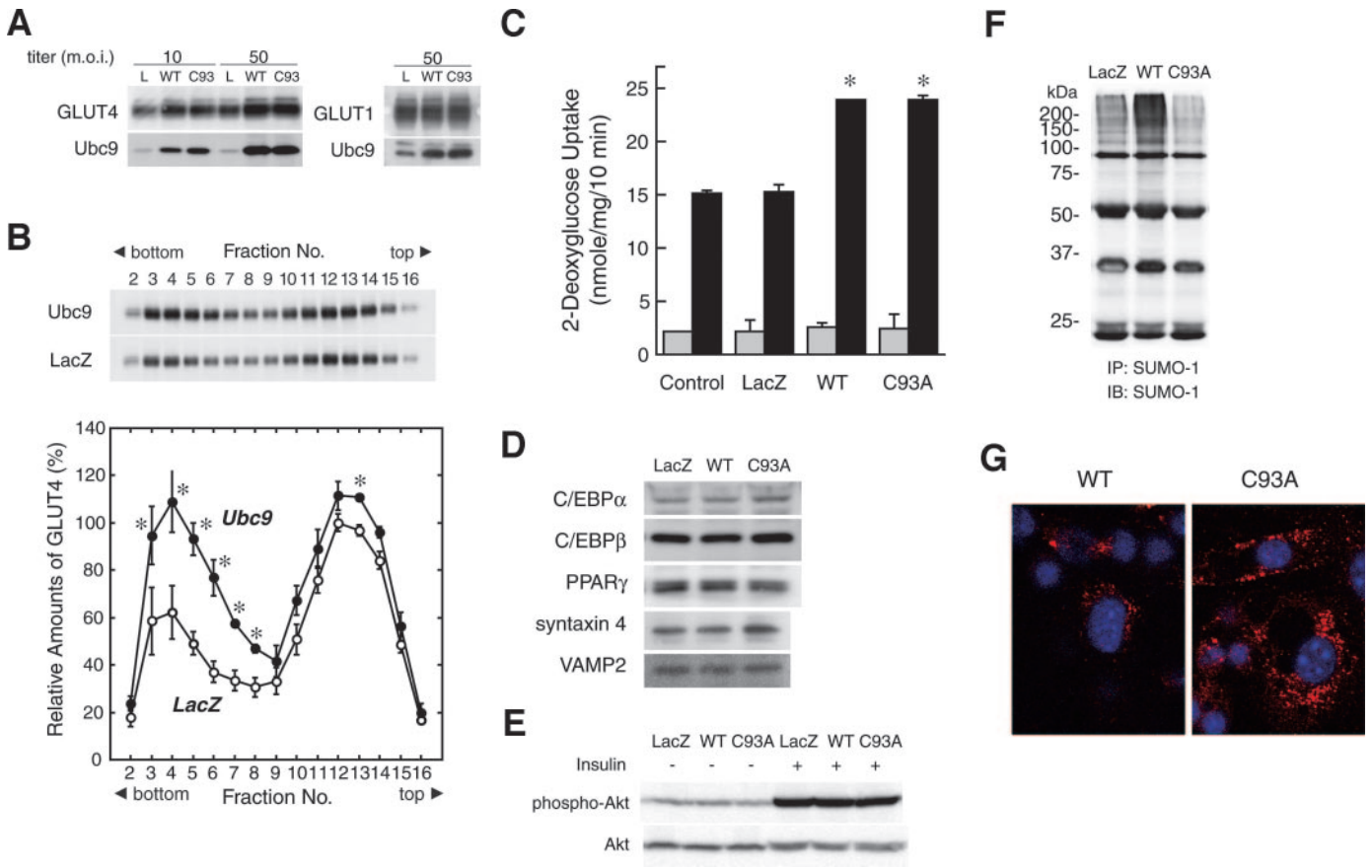

FIG. 3. Effects of overexpression of Ubc9 in 3T3-L1 adipocytes. *A*: Effects of Ubc9 overexpression on GLUT4 and GLUT1. Differentiated 3T3-L1 adipocytes were infected with adenoviruses carrying LacZ (L), Ubc9 (WT), or Ubc9-C93A (C93) at the indicated virus titer (MOI) and incubated for 48 h. At the end of incubation, cells were lysed and subjected to immunoblotting for GLUT4, GLUT1, or Ubc9. *B*: Iodixanol gradient analysis of the subcellular distribution of GLUT4. 3T3-L1 adipocytes were infected with adenoviruses (at 50 MOI) carrying LacZ or Ubc9 and incubated for 48 h in DMEM with 10% FBS, followed by incubation in serum-free DMEM for 3 h. At the end of incubation, cells were homogenized and the LDM fraction was prepared, which was subjected to iodixanol gradient centrifugation. Fractions were collected and immunoblotted with anti-GLUT4 antibody (*upper panel*). The relative amounts of GLUT4 were quantified and shown as the percentage of the peak value of peak 2 in the LacZ cells (*lower panel*). Results are the mean ± SE ($n = 3$). *$P < 0.01$ (vs. LacZ). *C*: Effects of Ubc9 overexpression on insulin-stimulated glucose transport. Differentiated 3T3-L1 adipocytes in 12-well plates were infected without (control) or with adenoviruses (at 50 MOI) containing LacZ, Ubc9, or Ubc9-C93A and incubated for 48 h. Then, cells were serum-starved for 3 h before stimulation without or with 100 nmol/l insulin for 30 min and subjected to the measurement of glucose transport activity. Data were shown as the mean ± SE ($n = 4–6$). *$P < 0.01$ (vs. plus insulin value of control cells). *D*: Effects of Ubc9 overexpression on transcription factors and SNAREs. The cell lysates prepared as in *A* were subjected to immunoblotting for PPARγ, C/EBPα and β, syntaxin 4, and VAMP-2. *E*: Effect of Ubc9 overexpression on insulin-stimulated Akt phosphorylation. 3T3-L1 adipocytes were infected with adenoviruses as in *A* before stimulation without or with 100 nmol/l insulin for 15 min. Then, cells were lysed and subjected to immunoblotting with anti-Akt and anti–phospho-Akt antibodies. *F*: Detection of SUMOylated proteins in 3T3-L1 adipocytes. Cells were infected with adenoviruses (at 50 MOI) containing LacZ, Ubc9, or Ubc9-C93A and incubated for 48 h. Then, cells were lysed in a buffer containing 25 mmol/l Tris/Cl, pH 8.0, 150 mmol/l NaCl, 1% NP-40, 0.1% SDS, 0.5% sodium deoxycholate, 1 mmol/l DTT, 5 mmol/l EDTA, 10 mmol/l *N*-methylmaleimide, 0.2 mmol/l iodoacetic acid, and complete protease inhibitor cocktail and subjected to immunoprecipitation and immunoblotting with anti–SUMO-1 antibody. *G*: Confocal images of the subcellular distribution of wild-type and C93A mutant Ubc9 in 3T3-L1 adipocytes. Differentiated adipocytes were infected with adenovirus containing Ubc9 or Ubc9-C93A and incubated for 48 h. Ubc9 (red) and the nuclei (blue) were visualized with anti-Ubc9 antibody and 4′,6-diamidino-2-phenylindole (DAPI), respectively.

nescent image analyzer (Fuji Photo Film). The intensities of the blots were quantified with Image Gauge software.

Immunofluorescence microscopy. 3T3-L1 adipocytes on cover slips were fixed with 3% (wt/vol) paraformaldehyde, immunostained with anti-GLUT4 (1:1,000), anti-Ubc9 (1:1,000), or anti-Syntaxin6 (1:1,000) antibodies and Alexa Fluor488- or Alexa Fluor 568-conjugated secondary antibodies (1:1,000) and observed by laser confocal microscopy as described previously (21,23).

Glucose transport assay. Cells in a 12-well culture dish were serum-starved for 3 h and incubated in Buffer A (25 mmol/l Krebs-Ringer Hepes, pH 7.4, containing 0.4% BSA and 3 mmol/l sodium pyruvate) for 1 h at 37°C, followed by stimulation with insulin (100 nmol/l) for 30 min. Cells were then incubated with 0.1 mmol/l 2-[1,2-^{3}H]deoxy-D-glucose (0.8 μCi/well) for 10 min. Nonspecific uptake was measured in the presence of 1 μmol/l cytochalasin B. At the end of incubation, cells were washed with ice-cold Buffer A and lysed in 0.4% SDS. The radioactivity in the lysate was counted with a scintillation counter.

Statistics. Data are expressed as means ± SE for the number of experiments indicated. Statistical significance between means was evaluated by the Student's *t* test.

RESULTS

As shown in Fig. 1*A* and *B*, the protein and mRNA levels of Ubc9 increased with differentiation of 3T3-L1 cells. In differentiated 3T3-L1 adipocytes, Ubc9 was found in both the soluble and membrane fractions (Fig. 1*C*). In the latter, Ubc9 was found predominantly in the LDM fraction, which was not affected with insulin stimulation. Immunofluorescence staining showed a concentration of Ubc9 in the perinuclear region colocalized with GLUT4 (Fig. 1*D*) as well as Syntaxin6 (Fig. 1*E*), suggesting that Ubc9 is mainly associated with TGN.

Next we examined the relevance of the subcellular targeting of GLUT4 to the insulin sensitivity of glucose transport. As shown in Fig. 2*A*, insulin stimulated glucose transport 7.2-fold in 3T3-L1 adipocytes, whereas its effects

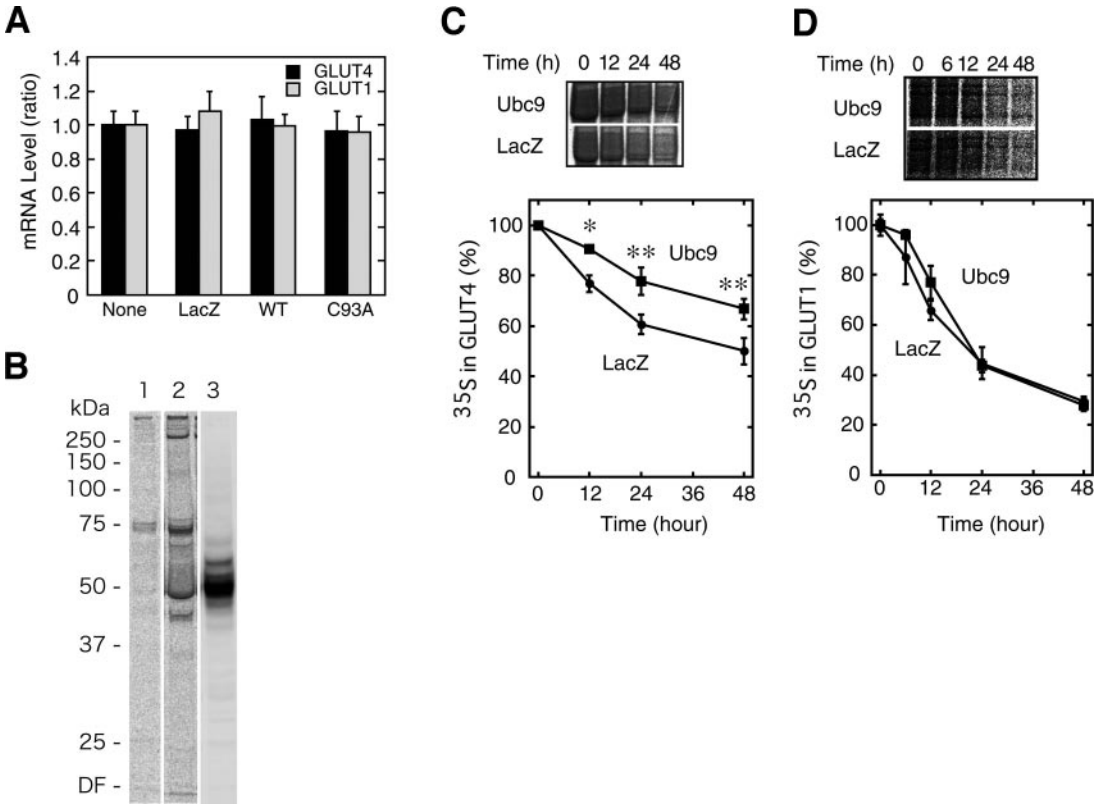

FIG. 4. Ubc9 overexpression retards GLUT4 degradation. *A*: Effects of Ubc9 overexpression on the mRNA levels of GLUT4 and GLUT1. Differentiated 3T3-L1 adipocytes were infected without (none) or with adenovirus (at 50 MOI) containing LacZ, Ubc9 (WT), or Ubc9-C93A (C93A) and incubated for 48 h. Cells were lysed and the mRNA levels of GLUT4 and GLUT1 measured by real-time RT-PCR as described in RESEARCH DESIGN AND METHODS. *B*: Identification of GLUT4 band in autoradiogram. 3T3-L1 adipocytes were pulse labeled with [^{35}S]methionine for 12 h. Then, cells were lysed and GLUT4 immunoprecipitated from the cell lysate and subjected to autoradiography as described in RESEARCH DESIGN AND METHODS. Representative autoradiogram of immunoprecipitates with nonimmune (*lane 1*) or anti-GLUT4 serum (*lane 2*). Lysate of nonlabeled cells were immunoblotted with anti-GLUT4 antibody (*lane 3*). *C* and *D*: Effects of Ubc9 overexpression on GLUT4 (*C*) and GLUT1 (*D*) turnover in 3T3-L1 adipocytes. Differentiated 3T3-L1 adipocytes were infected with adenovirus containing LacZ or Ubc9 and incubated for 24 h before pulse labeling with [^{35}S]methionine for 12 h. Then, cells were washed and chased in fresh medium for the indicated periods. At the end of incubation, GLUT4 or GLUT1 was immunoprecipitated from the cell lysate and subjected to autoradiography as described in RESEARCH DESIGN AND METHODS. *Upper panels*: Representative autoradiogram data. *Lower panels*: ^{35}S radioactivities in the GLUT4 or GLUT1 bands expressed as the percentage of the initial value. Results are shown as the mean ± SE (n = 4). *P < 0.05; **P < 0.01 (vs. LacZ).

were 1.3- and 1.5-fold in CHO cells expressing the insulin receptor (CHO-IR) and CHO-IR-GLUT4 cells, respectively. Thus, overexpression of GLUT4 in CHO-IR cells insignificantly potentiated the insulin responsiveness of glucose transport. To analyze the subcellular distribution of GLUT4, we separated the LDM fractions from 3T3-L1 adipocytes or CHO-IR-GLUT4 cells by iodixanol gradient centrifugation (24). As shown in Fig. 2*B*, two distinct GLUT4-containing membrane peaks (peaks 1 and 2) were resolved from the LDM fraction of 3T3-L1 adipocytes. Insulin recruited GLUT4 predominantly from peak 1, although the hormone also recruited GLUT4 from peak 2 to a lesser degree. By contrast, GLUT4 was found mainly in the lighter peak (peak 2) in CHO-IR-GLUT4 cells. Peak 2 coincided with the proteins resident in the endosomes (GLUT1, the transferrin receptor, and Rab4) and the TGN (syntaxin 6 and sortilin), whereas peak 1 was almost devoid of those proteins (Fig. 2*C*). Thus, peak 1 would correspond to the insulin-responsive GSC sequestered from the recycling compartments. This peak was absent before differentiation of 3T3-L1 adipocyte, since GLUT4-myc7-GFP was targeted exclusively to peak 2 in 3T3-L1 preadipocytes (Fig. 2*D*), in which the fold stimulation with insulin of glucose transport was 1.6-fold (data not shown). Thus, the insulin responsiveness of glucose transport apparently depends on the targeting of GLUT4 to GSC. Ubc9 coincided with peak 2 but not peak 1 in 3T3-L1 adipocytes (Fig. 2*E*). Although an intense band of Ubc9 was also found in fraction 2, GLUT4 was not present in this fraction, and its significance is unclear.

Next, we overexpressed Ubc9 in 3T3-L1 adipocytes using adenovirus vector and analyzed the GLUT4 amount and subcellular distribution as well as the glucose transport activity. As shown in Fig. 3*A*, overexpression of Ubc9 significantly increased GLUT4 amount (by ~60% at 50 MOI) without affecting GLUT1, the amount of which was not altered even at 72 and 96 h after infection (data not shown). Iodixanol gradient analyses demonstrated that although GLUT4 was increased in both peaks, the increment was significantly larger in peak 1 than 2, indicating that GLUT4 was preferentially targeted to GSC by Ubc9 overexpression (Fig. 3*B*). These changes were accompanied with potentiation of the insulin-responsive glucose transport by ~60% (Fig. 3*C*). Ubc9 overexpression did not affect the amounts of PPARγ and C/EBPα and β, the transcription factors involved in adipocyte differentiation (25,26), or those of syntaxin 4 and VAMP-2, the soluble *N*-ethylmaleimide-sensitive factor attachment protein receptor (SNARE) proteins implicated in GLUT4 translocation (3) (Fig. 3*D*). Likewise, the insulin-stimulated Akt phosphorylation was not altered (Fig. 3*E*). Ubc9 overex-

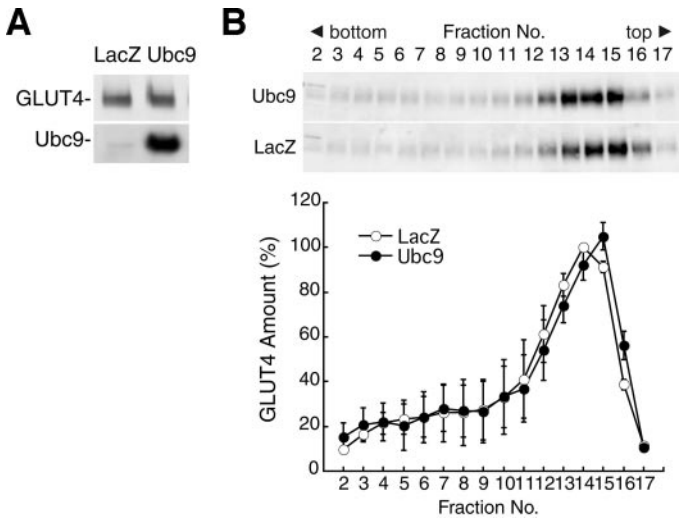

FIG. 5. Effects of Ubc9 overexpression in CHO-IR-GLUT4 cells. *A*: CHO-IR-GLUT4 cells were infected with adenoviruses (at 50 MOI) containing LacZ or Ubc9 and incubated for 48 h. At the end of incubation, cells were lysed and subjected to immunoblotting for GLUT4 and Ubc9. *B*: The LDM fractions were prepared from CHO-IR-GLUT4 cells infected with adenoviruses as in *A* and subjected to iodixanol gradient centrifugation. Fractions were collected and analyzed by immunoblotting with anti-GLUT4 antibody. *Upper panel*: Representative immunoblot data. *Lower panel*: Relative amounts of GLUT4 expressed as the percentage of the peak value in the LacZ cells. Results are shown as the mean ± SE (n = 3).

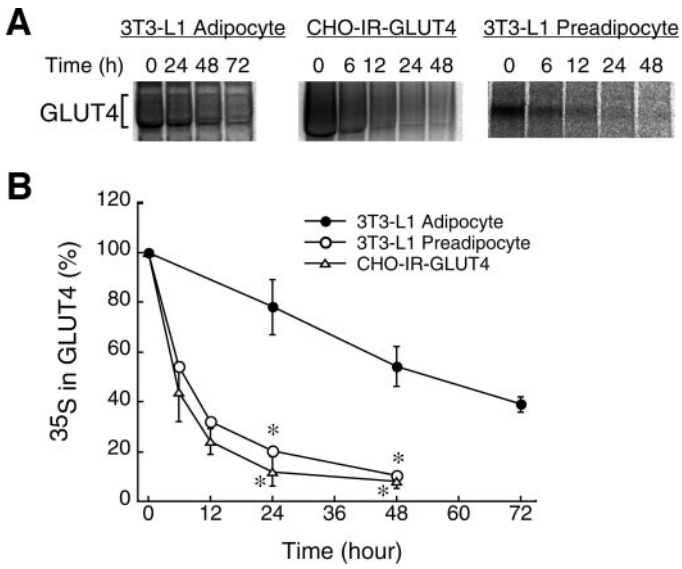

FIG. 6. GLUT4 turnover in 3T3-L1 adipocytes and preadipocytes and CHO-IR-GLUT4 cells. 3T3-L1 adipocytes, 3T3-L1 preadipocytes expressing GLUT4-myc7-GFP, and CHO-IR-GLUT4 cells were pulse labeled with [^{35}S]methionine for 12 h. After washing, cells were incubated in fresh medium for the indicated periods. At the end of incubation, GLUT4 was immunoprecipitated as described in RESEARCH DESIGN AND METHODS. The proteins were eluted and subjected to SDS-PAGE and autoradiography. *A*: Representative autoradiogram data from three independent experiments. *B*: Radioactivities in the GLUT4 bands expressed as the percentage of the initial value. Results are the means ± SE (n = 3). *P < 0.01 (vs. 3T3-L1 adipocyte).

pression did not significantly affect IRAP, syntaxin 6, or M6PR (data not shown).

Unexpectedly, overexpression of a catalytically inactive mutant of Ubc9 (Ubc9-C93A), which substitutes cystein[93] in the active site with alanine, showed the effects indistinguishable from those of wild-type Ubc9 (Fig. 3*A* and *C*). Since wild-type Ubc9 enhanced but Ubc9-C93A diminished the SUMOylation of cellular proteins in 3T3-L1 adipocytes (Fig. 3*F*), Ubc9-C93A likely works as a dominant interfering mutant for SUMOylation. Both wild-type and C93A mutant Ubc9 showed mainly cytoplasmic distribution with perinuclear accumulation (Fig. 3*G*). These results indicate that Ubc9 regulates GLUT4 and glucose transport by a mechanism independent of the SUMO-conjugation activity.

Next we investigated the mechanisms of GLUT4 upregulation by Ubc9 in 3T3-L1 adipocytes. As shown in Fig. 4*A*, neither wild-type nor mutant Ubc9 affected the mRNA levels of GLUT4 and GLUT1. By contrast, [^{35}S]methionine pulse-and-chase analyses revealed a significant delay in GLUT4 but not GLUT1 degradation by overexpression of Ubc9 (Fig. 4*C* and *D*). These data indicate that Ubc9 upregulates GLUT4 by retarding its degradation.

We also examined the effects of Ubc9 overexpression in CHO-IR-GLUT4 cells that do not possess GSC. As shown in Fig. 5, overexpression of Ubc9 neither increased GLUT4 nor stimulated generation of peak 1 in CHO-IR-GLUT4 cells. Thus, the ability of Ubc9 to increase GLUT4 may be cell type dependent and may require the existence of GSC, raising the possibility that GLUT4 turnover may be affected by its subcellular targeting.

To examine this possibility, we measured the half-life of GLUT4 protein in 3T3-L1 adipocytes and preadipocytes and CHO-IR-GLUT4 cells. As depicted in Fig. 6, the half-life of GLUT4 was ~50 h in 3T3-L1 adipocytes, whereas it was markedly shortened to ~6 h in 3T3-L1 preadipocytes and CHO-IR-GLUT4 cells. These results are consistent with the notion that GLUT4 turnover may become slower by targeting to GSC sequestered away from the recycling pathway (e.g., in 3T3-L1 adipocytes), while continuous residency in the recycling pathway may accelerate its degradation (e.g., in 3T3-L1 preadipocytes and CHO-IR-GLUT4 cells).

To further explore the relationship between the subcellular targeting and turnover of GLUT4, we examined whether continuous discharge of GLUT4 into the recycling pathway from GSC accelerates its degradation in 3T3-L1 adipocytes. Previous observations have indicated that insulin causes GLUT4 discharge from the storage compartment into the recycling pathway. Thus, an immuno-electron microscopic study has demonstrated an appearance of GLUT4 in the endosomes after insulin stimulation (11). By using a potent inhibitor of GLUT4 endocytosis, we reported that insulin induces a shift of GLUT4 from the retention pool to the recycling pathway in rat adipocytes (20). Furthermore, by expressing hemagglutinin-tagged GLUT4, two studies have shown a dose-dependent release of GLUT4 by insulin into the recycling pathway in 3T3-L1 adipocytes (27,28). As illustrated in Fig. 7*A*, stimulation of 3T3-L1 adipocytes with 500 nmol/l insulin for 12 h caused a reduction in GLUT4 amount by 40–50%, which was considerably prevented with lysosomal inhibitors (chloroquine and bafilomycin A_1) but not with calpain inhibitors (*N*-acetyl-Leu-Leu-Met-CHO [ALLM] and calpeptin). Intriguingly, the insulin effect was also blocked with proteasome inhibitors (lactacystin and MG132), suggesting that the ubiquitin-proteasome system may be involved in the insulin-induced GLUT4 degradation. Since bafilomycin A_1 and MG132 decreased rather than increased the GLUT4 mRNA level (Fig. 7*B*), their protective effects on GLUT4 did not derive from increased synthesis of GLUT4. These data suggest that insulin accelerates GLUT4 degradation by facilitating its sorting to the lysosomes. Of note, bafilo-

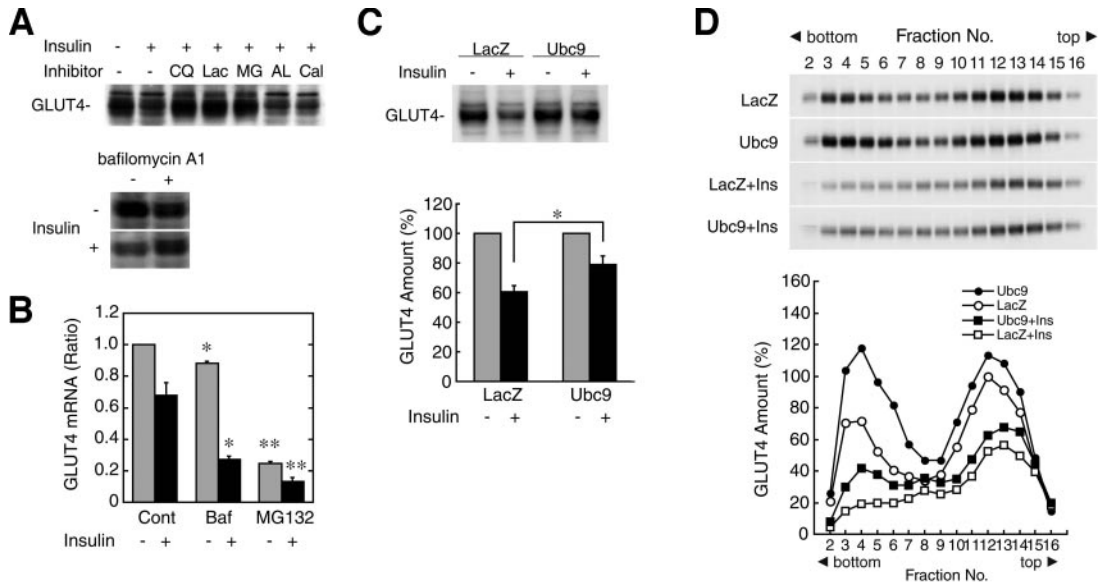

FIG. 7. Effects on chronic insulin stimulation on GLUT4. *A*: 3T3-L1 adipocytes were stimulated with or without insulin (500 nmol/l) for 12 h in the absence or presence of chloroquine (10 μmol/l), lactacystin (10 μmol/l), MG132 (20 μmol/l), ALLM (10 μmol/l), calpeptin (10 μmol/l), or bafilomycin A_1 (800 nmol/l). Then, cells were lysed and subjected to immunoblotting with anti-GLUT4 antibody. AL, ALLM; Baf, bafilomycin A_1; Cal, calpeptin; CQ, chloroquine; Lac, lactacystin; MG, MG132. *B*: Effects of bafilomycinA_1 or MG132 on the GLUT4 mRNA level. 3T3-L1 adipocytes were treated with bafilomycin A_1 (Baf) (800 nmol/l) or MG132 (20 μmol/l) for 12 h in the absence or presence of 500 nmol/l insulin, and mRNA level of GLUT4 was measured by real-time RT-PCR. Results are shown as the means ± SE (n = 4). *P < 0.01; **P < 0.001 (vs. control values for minus or plus insulin). *C*: Effects of Ubc9 overexpression on GLUT4 downregulation by chronic insulin stimulation. 3T3-L1 adipocytes were infected with adenoviruses containing LacZ or Ubc9 (at 50 MOI) and incubated for 36 h before stimulation with 500 nmol/l insulin for 12 h. At the end of incubation, cells were lysed and subjected to immunoblotting for GLUT4. *Upper panel*: Representative immunoblot data. *Lower panel*: Relative amounts of GLUT4 expressed as the percentage of the initial value. Results are the means ± SE (n = 4). *P < 0.01 (vs. plus insulin value in LacZ cells). *D*: Iodixanol gradient analysis of the GLUT4 distribution. 3T3-L1 adipocytes were infected with adenoviruses containing LacZ or Ubc9 and incubated as in *B* before stimulation without or with insulin (500 nmol/l) for 12 h. Then cells were serum starved for 3 h before homogenization and the LDM fractions prepared. The LDM fractions were separated by iodixanol gradient centrifugation. Fractions were collected from the bottom of the gradient and immunoblotted with anti-GLUT4 antibody. *Upper panel*: Immunoblot data. *Lower panel*: Relative amounts of GLUT4 expressed as the percentage of the peak value of peak 2 in the control (LacZ) cells.

mycin A_1 had an insignificant effect on GLUT4 in the basal cells (Fig. 7*A*), suggesting that lysosomal sorting of GLUT4 may not efficiently take place without insulin. Ubc9 overexpression significantly antagonized the insulin-induced GLUT4 downregulation (Fig. 7*C*).

Chronic insulin stimulation also causes a depletion of GLUT4 in GSC in adipocytes (29). Thus, we examined the effect of Ubc9 overexpression on the GLUT4 distribution in 3T3-L1 adipocytes stimulated with insulin for 12 h. While GLUT4 was decreased in all of the fractions in control cells, the reduction was more prominent in peak 1 than 2 (Fig. 7*D*), which was partially prevented by Ubc9 overexpression.

Finally, we depleted Ubc9 by using siRNA in 3T3-L1 adipocytes. As shown in Fig. 8*A*, Ubc9 knockdown decreased GLUT4 by ~50%, which was accompanied by its depletion in GSC (Fig. 8*B*), and accelerated GLUT4 degradation (Fig. 8*C*), while IRAP was less affected (by 20%). Intriguingly, Ubc9 knockdown also reduced the TGN-resident proteins such as sortilin, syntaxin 6, and M6PR but did not affect the endosomal recycling proteins (GLUT1 and the transferrin receptor), suggesting that Ubc9 may regulate the fate of TGN-derived vesicles (see DISCUSSION). Ubc9 knockdown attenuated the insulin-responsive glucose transport by ~35% (Fig. 8*D*).

DISCUSSION

The present study unveiled a novel regulatory mechanism of the insulin sensitivity of glucose transport in adipocyte. First, Ubc9 is a pivotal regulator of the subcellular targeting and turnover of GLUT4. This was shown by modulating the Ubc9 expression level in 3T3-L1 adipocytes. Overexpression of Ubc9 increased GLUT4 by retarding its degradation and promoted its targeting to GSC, both of which in concert potentiated the insulin responsiveness of glucose transport. By contrast, knockdown of Ubc9 produced the opposite effects. Neither overexpression nor knockdown of Ubc9 affected the amount of GLUT1, another glucose transporter isoform expressed in 3T3-L1 adipocytes. Thus, Ubc9 regulates the insulin responsiveness of glucose transport mainly through modulation of the amount and subcellular targeting of GLUT4. Additionally, Ubc9 overexpression antagonized the downregulation and aberrant targeting of GLUT4 induced by chronic insulin stimulation in 3T3-L1 adipocytes. Thus, Ubc9 plays a critical role under the physiological and pathological conditions.

While Ubc9 shows apparently dual effects on GLUT4 turnover and targeting, these two effects may relate to each other. Since inhibition of GLUT4 degradation with bafilomycin A_1 or MG132 did not promote GLUT4 targeting to GSC (our unpublished observation), inhibition of GLUT4 degradation would not be the primary mechanism of the Ubc9 action. Alternatively, we speculate that Ubc9 may primarily promote GLUT4 targeting to GSC, which causes retardation of GLUT4 degradation (see below).

Another intriguing finding is that the turnover of GLUT4 seems to be dependent on its subcellular targeting. First, the alterations of GLUT4 targeting to GSC by Ubc9 overexpression or knockdown were accompanied with the changes in the turnover rate of GLUT4 in 3T3-L1 adipocytes. Second, insulin-induced continuous discharge of GLUT4 into the recycling pathway resulted in a downregu-

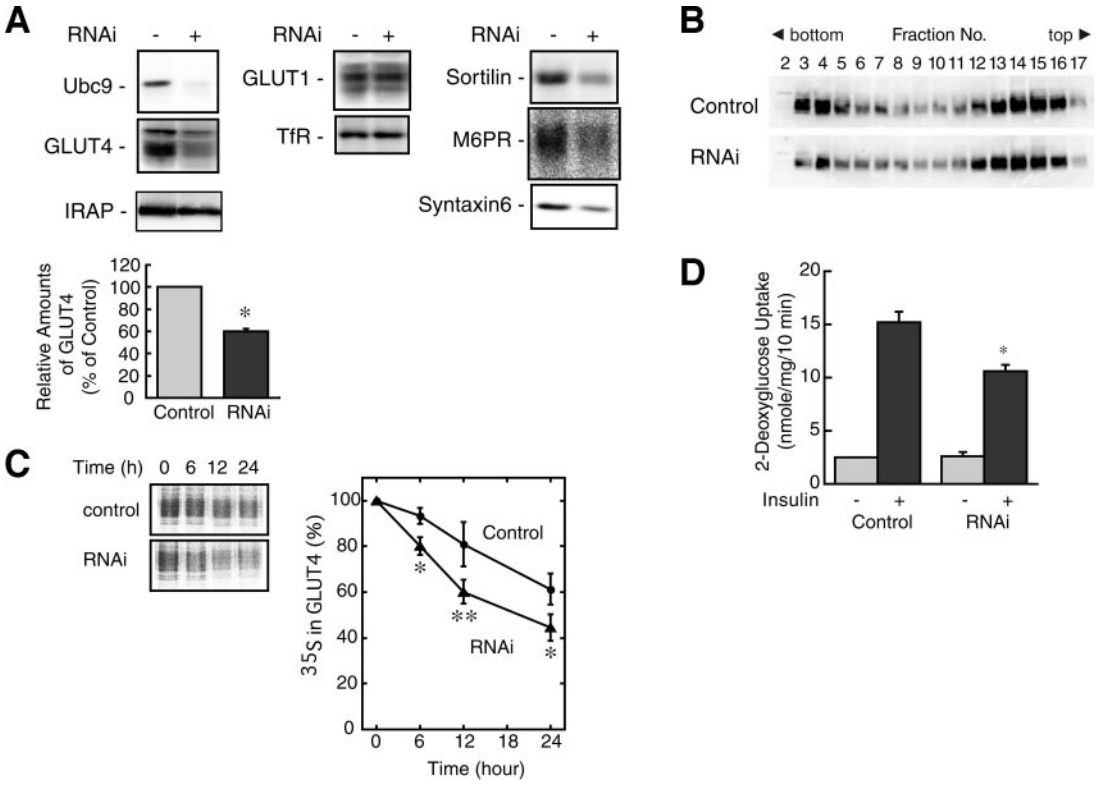

FIG. 8. Effects of Ubc9 knockdown in 3T3-L1 adipocytes. *A*: Effects of Ubc9knockdown on various proteins. Differentiated 3T3-L1 adipocytes were transfected with nonsilencing (control) or silencing (Ubc9) siRNA and incubated for 48 h. Then, cells were lysed and subjected to immunoblotting for the indicated proteins. The relative amounts of GLUT4 were shown in the lower bar graph. Results are shown as the means ± SE ($n = 3$). *$P < 0.01$. TfR, the transferring receptor; M6PR, the cation-dependent mannose-6-phosphate receptor. *B*: Iodixanol gradient analysis of GLUT4 distribution in Ubc9-depleted adipocytes. The LDM fractions were obtained from 3T3-L1 adipocytes transfected with siRNA as in *A* and were separated by iodixanol gradient centrifugation. Fractions were collected from the bottom of the gradient and subjected to immunoblotting for GLUT4. *C*: 3T3-L1 adipocytes were transfected with siRNA as in *A* and incubated for 24 h, followed by labeling with [^{35}S]methionine for 12 h. The cells were then incubated in fresh medium for the indicated periods. At the end of incubation, cells were lysed and GLUT4 immunoprecipitated before SDS-PAGE and autoradiography as described in RESEARCH DESIGN AND METHODS. *Left panel*: Representative immunoblot data. *Right panel*: Relative radioactivity in the GLUT4 bands expressed as the percentage of the initial value. Results are the mean ± SE ($n = 4$). *$P < 0.05$; **$P < 0.01$ (vs. control). *D*: The glucose transport activity in Ubc9-depleted adipocytes. 3T3-L1 adipocytes transfected with siRNA for 48 h as in *A* were further incubated in serum-free medium for 3 h before stimulation without or with 100 nmol/l insulin for 30 min, then the glucose transport activity was measured. Results are the means ± SE ($n = 6$). *$P < 0.01$ (vs. plus insulin value in control cells).

lation of the transporter. Third, GLUT4 turnover was markedly accelerated in 3T3-L1 preadipocytes and CHO-IR-GLUT4 cells compared with 3T3-L1 adipocytes. In those cell types, GLUT4 is localized predominantly to the recycling pathway for lack of GSC. These observations are consistent with a model that continuous residency of GLUT4 in the recycling pathway accelerates its degradation by facilitated sorting to the lysosomes, while sequestration of the transporter in GSC from the recycling pathway retards its degradation. In agreement with our observations, Shi and Kandror (18) have recently reported that sortilin-promoted formation of GLUT4 storage vesicles markedly increases the stability of GLUT4 protein. Taking into account that the subcellular distribution GLUT4 changes more dynamically than GLUT1 with a variety of stimuli (e.g., insulin), GLUT4 turnover may be more vigorously affected by alteration in the subcellular localization than GLUT1. In fact, continuous stimulation with insulin of 3T3-L1 adipocytes reduced the half-life of GLUT4 from 50 to 15.5 h, while its effect on that of GLUT1 was less significant (from 19 to 15.5 h) (30).

Several questions remain to be answered as to the mechanisms by which Ubc9 regulates GLUT4 targeting and turnover. Since wild-type and the catalytically inactive mutant Ubc9 showed indistinguishable effects on GLUT4, Ubc9 would regulate GLUT4 targeting and turnover by a mechanism other than SUMOylation. The observations also contradict the idea that Ubc9 exerts the effects by SUMOylation of GLUT4 itself (19,31). Since knockdown of Ubc9 produced effects opposite to those of its overexpression, Ubc9 may regulate GLUT4 targeting through interaction with a putative target molecule(s).

The target molecule(s) of Ubc9 is unknown but may be among GLUT4 itself, GLUT4-associated molecules, or the components of the GLUT4 sorting machineries. While Ubc9 was previously reported to interact with a highly conserved sequence in the carboxyl-terminal domain of GLUT4 by the yeast two-hybrid system (19), this interaction is not specific to GLUT4 and has not been proved in the cellular level. Thus, although we do not preclude the possibility that Ubc9 may regulate GLUT4 sorting through the interaction with the transporter, the physiological significance of this interaction has yet to be investigated. On the other hand, Lalioti et al. (31) reported the dileucine ($L^{489}L^{490}$) motif-dependent interaction of GLUT4 with Daxx, a Fas binding protein, which also interacts with Ubc9. Since the GLUT4 interacting region and the Ubc9 interacting region of Daxx considerably overlap (amino acid residues 661–740 and 625–740, respectively), it is an intriguing possibility that Ubc9 may regulate GLUT4 trafficking by modifying the interaction of Daxx with GLUT4.

Alternatively, Ubc9 may interact with the sorting ma-

chinery that destines GLUT4 to either GSC or the lysosomes or with the tethering machinery that retains GLUT4 in GSC. The data from iodixanol gradient centrifugation and immunofluorescence microscopy revealed predominant localization of Ubc9 in TGN, suggesting TGN as a likely candidate for the site of Ubc9 action.

Recent studies have demonstrated that Golgi-localized, γ-ear-containing, Arf-binding protein (GGA) mediates formation of the insulin-responsive GLUT4 storage vesicles from TGN (32,33). Additionally, sortilin, a GGA-binding protein, has been reported to regulate formation of GLUT4 storage vesicles (18). Thus, Ubc9 may facilitate formation of GSC at TGN by interacting with such proteins. Alternatively, Ubc9 may redirect GLUT4 to GSC by preventing its sorting to the lysosomes. In this regard, Ubc9 knockdown caused a depletion of the TGN-resident proteins such as sortilin, syntaxin 6, and M6PR (Fig. 8). Since these proteins are found in immunopurified GLUT4-containing vesicles (24), Ubc9 may negatively regulate the lysosomal sorting of TGN-derived vesicles carrying GLUT4 and these TGN-resident proteins. Further study is apparently needed to address these issues.

In summary, by modulating the expression level of Ubc9, we have demonstrated that Ubc9 is a pivotal regulator of subcellular targeting and turnover of GLUT4 in adipocytes. Ubc9-regulated GLUT4 targeting to GSC may cause retardation of GLUT4 turnover, with consequent GLUT4 upregulation and potentiation of insulin-responsive glucose transport. Thus, Ubc9 plays an indispensable role in the acquisition and maintenance of insulin sensitivity of the glucose transport system in adipocytes.

ACKNOWLEDGMENTS

This work was supported by the 21st Century Centers of Excellence Program "Processing of Biosignals: Receptor Activation, Signal Transduction, Functional Expression and Animal Behaviors" and grant-in-aid from the Ministry of Education, Culture, Sports, Science and Technology of Japan.

We are grateful to Dr. René Bernards for the Ubc9 cDNA, Dr. Harvey F. Lodish for the pB-GLUT4-myc7-GFP retrovirus vector, and Dr. Toshio Kitamura for Platinum-E cells.

REFERENCES

1. Cushman SW, Wardzala LJ: Potential mechanism of insulin action on glucose transport in the isolated rat adipose cell: apparent translocation of intracellular transport systems to the plasma membrane. *J Biol Chem* 255:4758–4762, 1980
2. Suzuki K, Kono T: Evidence that insulin causes translocation of glucose transport activity to the plasma membrane from an intracellular storage site. *Proc Natl Acad Sci U S A* 77:2542–2545, 1980
3. Bryant NJ, Govers R, James DE: Regulated transport of the glucose transporter GLUT4. *Nat Rev Mol Cell Biol* 3:267–277, 2002
4. Holman GD, Sandoval IV: Moving the insulin-regulated glucose transporter GLUT4 into and out of storage. *Trends Cell Biol* 11:173–179, 2001
5. Mitsumoto Y, Burdett E, Grant A, Klip A: Differential expression of the GLUT1 and GLUT4 glucose transporters during differentiation of L6 muscle cells. *Biochem Biophys Res Commun* 175:652–659, 1991
6. Garcia de Herreros A, Birnbaum MJ: The acquisition of increased insulin-responsive hexose transport in 3T3–L1 adipocytes correlates with expression of a novel transporter gene. *J Biol Chem* 264:19994–19999, 1989
7. Haney PM, Slot JW, Piper RC, James DE, Mueckler M: Intracellular targeting of the insulin-regulatable glucose transporter (GLUT4) is isoform specific and independent of cell type. *J Cell Biol* 114:689–699, 1991
8. Hudson AW, Ruiz M, Birnbaum MJ: Isoform-specific subcellular targeting of glucose transporters in mouse fibroblasts. *J Cell Biol* 116:785–797, 1992
9. Shibasaki Y, Asano T, Lin JL, Tsukuda K, Katagiri H, Ishihara H, Yazaki Y, Oka Y: Two glucose transporter isoforms are sorted differentially and are expressed in distinct cellular compartments. *Biochem J* 281:829–834, 1992
10. Lampson MA, Schmoranzer J, Zeigerer A, Simon SM, McGraw TE: Insulin-regulated release from the endosomal recycling compartment is regulated by budding of specialized vesicles. *Mol Biol Cell* 12:3489–3501, 2001
11. Slot JW, Geuze HJ, Gigengack S, Lienhard GE, James DE: Immunolocalization of the insulin regulatable glucose transporter in brown adipose tissue of the rat. *J Cell Biol* 113:123–135, 1991
12. Malide D, Ramm G, Cushman SW, Slot JW: Immunoelectron microscopic evidence that GLUT4 translocation explains the stimulation of glucose transport in isolated rat white adipose cells. *J Cell Sci* 113:4203–4210, 2000
13. Livingstone C, James DE, Rice JE, Hanpeter D, Gould GW: Compartment ablation analysis of the insulin-responsive glucose transporter (GLUT4) in 3T3–L1 adipocytes. *Biochem J* 315:487–495, 1996
14. Martin LB, Shewan A, Millar CA, Gould GW, James DE: Vesicle-associated membrane protein 2 plays a specific role in the insulin-dependent trafficking of the facilitative glucose transporter GLUT4 in 3T3–L1 adipocytes. *J Biol Chem* 273:1444–1452, 1998
15. Calderhead DM, Kitagawa K, Tanner LI, Holman GD, Lienhard GE: Insulin regulation of the two glucose transporters in 3T3–L1 adipocytes. *J Biol Chem* 265:13801–13808, 1990
16. Tanner LI, Lienhard GE: Insulin elicits a redistribution of transferrin receptors in 3T3–L1 adipocytes through an increase in the rate constant for receptor externalization. *J Biol Chem* 262:8975–8980, 1987
17. Appell KC, Simpson IA, Cushman SW: Characterization of the stimulatory action of insulin on insulin-like growth factor II binding to rat adipose cells: differences in the mechanism of insulin action on insulin-like growth factor II receptors and glucose transporters. *J Biol Chem* 263:10824–10829, 1988
18. Shi J, Kandror KV: Sortilin is essential and sufficient for the formation of Glut4 storage vesicles in 3T3–L1 adipocytes. *Dev Cell* 9:99–108, 2005
19. Giorgino F, de Robertis O, Laviola L, Montrone C, Perrini S, McCowen KC, Smith RJ: The sentrin-conjugating enzyme mUbc9 interacts with GLUT4 and GLUT1 glucose transporters and regulates transporter levels in skeletal muscle cells. *Proc Natl Acad Sci U S A* 97:1125–1130, 2000
20. Shibata H, Suzuki Y, Omata W, Tanaka S, Kojima I: Dissection of GLUT4 recycling pathway into exocytosis and endocytosis in rat adipocytes: evidence that GTP-binding proteins are involved in both processes. *J Biol Chem* 270:11489–11495, 1995
21. Liu LB, Omata W, Kojima I, Shibata H: Insulin recruits GLUT4 from distinct compartments via distinct traffic pathways with differential microtubule dependence in rat adipocytes. *J Biol Chem* 278:30157–30169, 2003
22. Student AK, Hsu RY, Lane MD: Induction of fatty acid synthetase synthesis in differentiating 3T3–L1 preadipocytes. *J Biol Chem* 255:4745–4750, 1980
23. Omata W, Shibata H, Suzuki Y, Tanaka S, Suzuki T, Takata K, Kojima I: Subcellular distribution of GLUT4 in Chinese hamster ovary cells overexpressing mutant dynamin: evidence that dynamin is a regulatory GTPase in GLUT4 endocytosis. *Biochem Biophys Res Commun* 241:401–406, 1997
24. Hashiramoto M, James DE: Characterization of insulin-responsive GLUT4 storage vesicles isolated from 3T3–L1 adipocytes. *Mol Cell Biol* 20:416–427, 2000
25. Rosen ED, Spiegelman BM: PPARgamma: a nuclear regulator of metabolism, differentiation, and cell growth. *J Biol Chem* 276:37731–37734, 2001
26. Ramji DP, Foka P: CCAAT/enhancer-binding proteins: structure, function and regulation. *Biochem J* 365:561–575, 2002
27. Govers R, Coster AC, James DE: Insulin increases cell surface GLUT4 levels by dose dependently discharging GLUT4 into a cell surface recycling pathway. *Mol Cell Biol* 24:6456–6466, 2004
28. Coster AC, Govers R, James DE: Insulin stimulates the entry of GLUT4 into the endosomal recycling pathway by a quantal mechanism. *Traffic* 5:763–771, 2004
29. Maier VH, Gould GW: Long-term insulin treatment of 3T3–L1 adipocytes results in mis-targeting of GLUT4: implications for insulin-stimulated glucose transport. *Diabetologia* 43:1273–1281, 2000
30. Sargeant RJ, Paquet MR: Effect of insulin on the rates of synthesis and degradation of GLUT1 and GLUT4 glucose transporters in 3T3–L1 adipocytes. *Biochem J* 290:913–919, 1993
31. Lalioti VS, Vergarajauregui S, Pulido D, Sandoval IV: The insulin-sensitive glucose transporter, GLUT4, interacts physically with Daxx. Two proteins with capacity to bind Ubc9 and conjugated to SUMO1. *J Biol Chem* 277:19783–19791, 2002
32. Li LV, Kandror KV: Golgi-localized, gamma-ear-containing, Arf-binding protein adaptors mediate insulin-responsive trafficking of glucose transporter 4 in 3T3–L1 adipocytes. *Mol Endocrinol* 19:2145–2153, 2005
33. Watson RT, Khan AH, Furukawa M, Hou JC, Li L, Kanzaki M, Okada S, Kandror KV, Pessin JE: Entry of newly synthesized GLUT4 into the insulin-responsive storage compartment is GGA dependent. *Embo J* 23:2059–2070, 2004